Korean J. Chem. Eng., **30**(6), 1265-1271 (2013)
DOI: 10.1007/s11814-013-0063-2

Fabrication and modification of polyvinylchloride based heterogeneous cation exchange membranes by simultaneously using Fe-Ni oxide nanoparticles and Ag nanolayer: Physico-chemical and antibacterial characteristics

Akbar Zendehnam*,†, Mina Arabzadegan*, Sayed Mohsen Hosseini,†, Nasrin Robatmili*, and Sayed Siavash Madaeni*****

*Thin Film Laboratory, Department of Physic, Faculty of Science, Arak University, Arak 38156-8-8349, Iran
**Department of Chemical Engineering, Faculty of Engineering, Arak University, Arak 38156-8-8349, Iran
***Membrane Research Centre, Department of Chemical Engineering, Faculty of Engineering, Razi University, Kermanshah 67149, Iran
(*Received 21 February 2013 • accepted 20 April 2013*)

Abstract−Polyvinylchloride-blend-styrene butadiene rubber based nanocomposite cation exchange membranes were prepared by solution casting technique. Iron-oxide nanoparticles and Ag-nanolayer were simultaneously utilized as filler and surface modifier in membrane fabrication. The effects of Ag-nanolayer film thickness on membrane physico-chemical and antibacterial characteristics of nanocomposite PVC-blend-SBR/Iron-oxide nanoparticles were studied. SEM images showed membrane roughness decreasing by Ag nanolayer thickness increasing. Membrane charge density and selectivity declined by Ag nanolayer coating up to 5 nm in membranes and then showed increasing trend by more nanolayer thickness. Ionic flux also showed increasing trend. Membranes showed good ability in E-Coli removal. 20 nm Ag-nanolayer coated membrane showed better performance compared to others.

Key words: Cation Exchange Membrane, Fabrication/Modification, Ag Nanolayer/Fe-Ni Oxide Nanoparticles, Physico Chemical/Antibacterial Characteristic, Synergy Phenomenon

INTRODUCTION

Ion exchange membranes (IEMs) are widely utilized as active separators in diverse electrically driven processes. In IEMs, charged groups attached to polymer backbone are freely permeable to opposite sign ions under the influence of an electrical field [1,2]. Depending on the type of ionic groups attached to the membrane matrix, IEMs are classified into anion exchange and cation exchange ones [3,4]. IEMs are generally applied in treatment of ionic solutions, re-concentrating brine from seawater, desalting saline water, demineralization of whey, acid and alkali recovery and many more processes [5-7].

However, preparing inexpensive membranes with specially adapted physico-chemical characteristics may be a vital step in future chemical and treatment application [2]. Variation of functional groups, selection of different polymeric matrices, polymers blending, using of various additives such as metal/metal oxide nanoparticles in membrane matrix and surface modification by plasma treatment are important ways to obtain superior IEMs [2,8-19].

Fabrication of heterogeneous cation exchange membranes with appropriate physico-chemical properties for application in electrodialysis process related to water recovery and treatment was the primary target of the current research. For the purpose, polyvinychloride-blend-styrene butadiene rubber heterogeneous cation exchange membranes were prepared by solution casting techniques using cation exchange resin powder as functional groups agent. PVC is a flexible and durable polymer with suitable biological and chemical resistance. SBR is also a rubbery polymer with good permeability and appropriate abrasion resistance and aging stability. The use of these polymers and their blends as membrane binders can dedicate special selective characteristics in prepared membranes with respect to superior mechanical support of glassy polymers and toughness and high permeability of flexible rubbery ones [11,19-22]. Iron-nickel oxide nanoparticles and silver nanolayer were also employed as inorganic filler additive and surface modifier in membrane fabrication respectively in order to improve the IEMs physico-chemical and antibacterial characteristics. Ag nanolayer was deposited on membrane surface by magnetron sputtering method, which has many advantages such as good adhesion of film to substrate, uniformity, good and controllable deposition rate and high purity [19,23]. In recent years, the use of metal nanoparticles in polymeric matrix has been increased obviously. The use of metals against microorganisms can be considered very old for food preparing and preserving from pollution. Silver has been found to be non-toxic to humans at very small concentrations. The continuous release of silver ions enhances its antimicrobial efficacy [24-26]. In these times, silver nanoparticles have found diverse applications in the form of wound dressings, coatings for medical devices, textile, treating effluent and many more [27].

Iron-nickel oxide nanoparticles are also a new class of advanced materials with very interesting features and capacity such as superior magnetic, electrical and selective adsorption properties which also have been utilized in water treatment [11].

The effects of iron-nickel oxide nanoparticle and Ag nanolayer on the physico-chemical properties of prepared heterogeneous cat-

†To whom correspondence should be addressed.
E-mail: Sayedmohsen_Hosseini@yahoo.com, A-zendehnam@araku.ac.ir

ion exchange membranes were studied. During the experiments, sodium chloride was employed as ionic solution for the membrane characterization. The results are valuable for electro-membrane processes especially in electrodialysis process for water recovery and treatment.

MATERIALS AND METHODS

1. Materials

Polyvinylchloride (PVC, grade S-7054, high porosity, bulk density: 490 g/L, viscosity number: 105 cm^3/g) and styrene butadiene rubber (SBR, grade 1502, bound styrene: 22.5-24.5 wt%, ultimate elongation: 350% and modulus: 167-207 kg/cm^2) supplied by Bandar Imam Petrochemical Company (BIPC, Iran) were used as binders. Tetrahydrofuran was employed as solvent. Iron nickel oxide nanoparticle (Fe_2NiO_4, nano-powder, particle size<50 nm, 98% trace metals basis) by Aldrich as inorganic filler additive and cation exchange resin (Ion exchanger Amberlyst® 15, strongly acidic cation exchanger, H^+ form - more than 1.7 milli equivalent/g dry) by Merck Inc., Germany, were used in membrane preparation. Silver plate target with high purity (99.99%) was also used in nanolayer preparation. All other chemicals were supplied by Merck. Throughout the experiment, distilled water was used.

2. Preparation of Heterogeneous Cation Exchange Membranes

Heterogeneous cation exchange membranes were prepared by casting solution technique and phase inversion method. Resin particles were pulverized into fine particles in a ball mill and then sieved to the desired particle size (−300 +400 mesh). Membranes were prepared by dissolving the polymer binder ((PVC : SBR) (9 : 1) w/w) into THF solvent (THF : Polymer; (20 : 1) v/w) in a glass reactor equipped with a mechanical stirrer [2]. This was followed by dispersing a specific quantity of ground resin particle (resin : polymer; (1 : 1) w/w) as functional groups agents and iron nickel oxide nanoparticle as additive (8.0%wt [11]) in polymeric solution, respectively, as described earlier [10,11,19]. The mixture was mixed vigorously at room temperature to obtain a uniform particle distribution in the polymeric solution. In addition, for better dispersion of particles and breaking up their aggregates, the solution was sonicated with an ultrasonic instrument. Then, the mixture was cast onto a clean and dry glass plate at 25 °C. The membranes were dried at ambient temperature and immersed in distilled water. Membranes were pretreated by immersing in NaCl solution. The membrane thickness was measured by a digital caliper to maintain the membrane thickness around 80-100 μm.

3. Membrane Surface Modification by Plasma Treatment

Silver (Ag) nanoparticles/nanolayer was deposited on membranes surface by plasma treatment. For the purpose, a vacuum system (with base pressure 10^{-6} mbar) was employed (PLANAR MAGNETRON SPUTTERING MODEL-12" MSPT, HIND HIGH VACCUM CO. Private LTD. BANGLORE, INDIA) at 25 °C and 90 w power (DC MAGNETRON SUPPLY POWER MODEL-PS-2000). For plasma formation pure argon research grade (99.99%purity) was used in the range of $2\text{-}5\times10^{-2}$ mbar. Silver target (high purity, 99.99%) with 12.5 cm diameter and 3 mm thickness was made and used as a cathode for sputtering. The distance between silver (Ag) plate target and membranes (substrate) holder in plasma reactor during the process was kept at 12 centimeters. At this distance (optimum distance) a uniform film with good packing density was obtained. Different film thicknesses (5, 10, 15, 20 nm) were deposited on the membranes surface with constant deposition rate of 1.35 (nm/s).

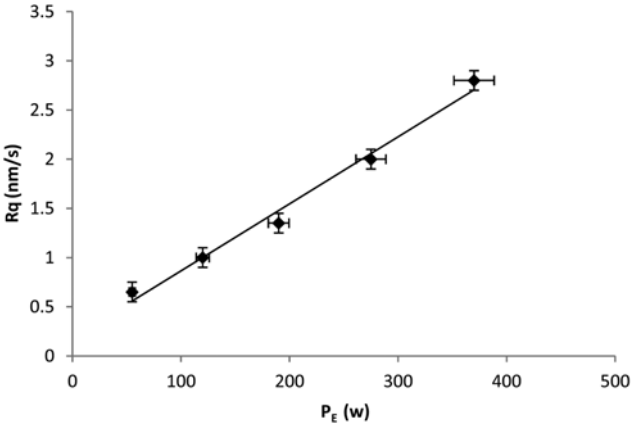

Fig. 1. Rate of deposition (R_q) versus electrical power (P_E).

The deposition rate of silver layer can be expressed as follows [23]:

$$R_q = k\frac{P_E}{pd},\quad P_E = VI \tag{1}$$

where R_q is the coating rate, V is voltage, P is gas pressure (Ar), d is the distance between target (Ag cathode) and anode (substrate holder), P_E is the electrical power (voltage time's current) and k is a constant which depends on type of gas and target material. The variation of deposition rate against electrical power is given (Fig. 1). A linear plot is obtained, as it was expected. In relation (1), k/pd is the slope that was fixed in this work.

Treating time was changed to adjust the Ag nanolayer thickness on the membrane surface (5-30 nm with ±2 nm instrument error). The target was pre-sputtered for 10 min with a moveable shutter placed in between the target and substrate. This shutter was also used to control the time of layer deposition. The coating procedure was carried out at 25 °C temperature.

4. Test Cells

The electrochemical property measurements for the membranes were carried out using the test cell (Fig. 2) as reported earlier [10,

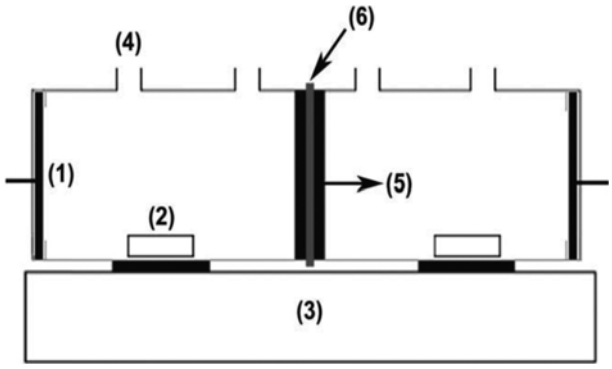

Fig. 2. Schematic diagram of test cell.

1. Pt electrode
2. Magnetic bar
3. Stirrer
4. Orifice
5. Rubber ring
6. Membrane

11,19]. The cell consists of two cylindrical compartments made of Pyrex glass which are separated by membrane. One side of each vessel was closed by Pt electrode supported with a piece of Teflon, and the other side was equipped with a piece of porous medium to support the membrane. For feeding and sampling purposes, the top of each compartment contained two orifices. To minimize the effect of boundary layer during experiments and to establish the concentration polarization on the vicinity of membrane's surface, both sections were stirred vigorously by magnetic stirrers.

5. Membrane Characterization

5-1. Morphological Studies

The behavior of prepared membranes is closely related to their structure, especially the spatial distribution of ionic sites [28]. The structure of prepared membranes was examined by scanning optical microscopy (SOM Olympus, model IX 70) in transmission mode with light going through the membrane. The surface of the films was also analyzed by scanning electron microscope (SEM, S360 Cambridge 1990).

5-2. Membrane Potential, Transport Number and Permselectivity

Membrane potential is the algebraic sum of Donnan and diffusion potentials. The magnitude of this parameter depends on the electrical characteristic of the membrane along with the nature and concentration of the electrolyte solution [12,29,30]. This parameter was evaluated for the equilibrated membrane with unequal concentrations of sodium chloride (C_1=0.1 M, C_2=0.01 M @ ambient temperature) on either side of the membrane using a two-cell glassy apparatus shown in Fig. 2. The developed potential difference across the membrane was measured by connecting both compartments and using saturated calomel electrode (through KCl bridges) and digital auto multi-meter. The membrane potential ($E_{measure}$) generated is expressed using Nernst equation [10-13,28-30] as follows:

$$E_{measure} = (2t_i^m - 1)\left(\frac{RT}{nF}\right)Ln\left(\frac{a_1}{a_2}\right) \tag{2}$$

where t^m is the transport number of counter ions in the membrane phase, R is the gases constant, T is the temperature, n is the electrovalence of counter ion and a_1, a_2 are solutions electrolyte activities in contact with both surfaces determined using the Debye-Hackle limiting law. The ionic permselectivity of membranes also is quantitatively expressed based on the migration of counter-ion through the ion-exchange membrane [10-13,28-30].

$$Ps = \frac{(t_i^m - t_0)}{(1 - t_0)} \tag{3}$$

where t_0 is the transport number of the counter ions in solution [31].

The ionic permselectivity (Ps) is a term used to define the preferential permeation of certain ionic species through ion-exchange membranes.

The concentration of fixed charge on the membrane surface (Y) also has been expressed in terms of permselectivity as follows [12,29]:

$$Y = \frac{2C_{mean}Ps}{\sqrt{(1 - Ps^2)}} \tag{4}$$

where C_{mean} is the mean concentration of electrolytes.

5-3. Membrane Ionic Permeability and Flux

The ionic permeability and flux of ions were measured by using the test cell as reported earlier [10,11]. A 0.1 M NaCl solution was placed on one side of the cell and a 0.01 M solution on its other side. A DC electrical potential with an optimal constant voltage was applied across the cell with stable platinum electrodes. To ensure the equilibrium condition in two solution-membrane interfacial zones and to minimize the effect of boundary layers, both sections were stirred vigorously by magnetic stirrers.

$$2Cl^- \Rightarrow Cl_2 \uparrow + 2e^- \quad \text{(Anodic reaction)}$$

$$2H_2O + 2e^- \Rightarrow H_2 \uparrow + 2OH^- \quad \text{(Cathodic reaction)}$$

According to the reactions that occurred, the produced hydroxide ions increase the pH of cathodic region. The pH changes were measured with a digital pH-meter (Jenway, Model: 3510). According to first Fick's law, the flux of ions through the membrane can be expressed as follows [10,11,13,19,28]:

$$N = P\frac{C_1 - C_2}{d} \tag{5}$$

where, P is coefficient diffusion of ions, d is membrane thickness, N is ionic flux and C is the cations concentration in the compartments.

$$N = -\frac{V}{A} \times \frac{dC_1}{dt} = P\frac{C_1 - C_2}{d} \tag{6}$$

$$C_1^0 = 0.1M,\ C_2^0 = 0.01M,\ C_1 + C_2 = C_1^0 + C_2^0 = 0.11M \tag{7}$$

where, A is the membrane surface area. Integrating of Eq. (7) was as follows:

$$\ln\frac{(C_1^0 + C_2^0 - 2C_2)}{(C_1^0 - C_2^0)} = -\frac{2PAt}{Vd} \tag{8}$$

The diffusion coefficient and flux of cations in membrane phase are calculated from Eq. (9) considering pH changes measurements in cathodic section.

5-4. Electrical Property of Ag Thin Film Coated Membrane

To study the influence of Ag thickness on the electrical resistively of nano-layers coated on membranes a four-probe (INDOSAW-Model SK012) was employed. The increase of electrical conductivity improves the interactions of ions with membrane surface and also the intensity of uniform electrical field around the membrane surface.

5-5. Antibacterial Effect

Silver nanoparticle shows good anti-bacterial and anti-microbial characteristic and so has been utilized extensively in medical and water industries. In this work the anti-bacterial effect of thin silver-coated membrane was studied using the optical density method. For these measurements a spectrophotometer (Elegant Thch.Cecil series 400, CE 4400) with wavelength 600 nm was employed.

RESULTS AND DISCUSSION

1. Morphological Studies

The SOM and SEM (3D) images of prepared membranes are shown in Figs. 3 and 4, respectively. The non-conducting area (polymer binder) and conducting ion exchange areas (resin particles) are clearly seen in SOM images. Resin particles are uniformly distributed in the prepared membranes. Also, deposited silver nanolayer

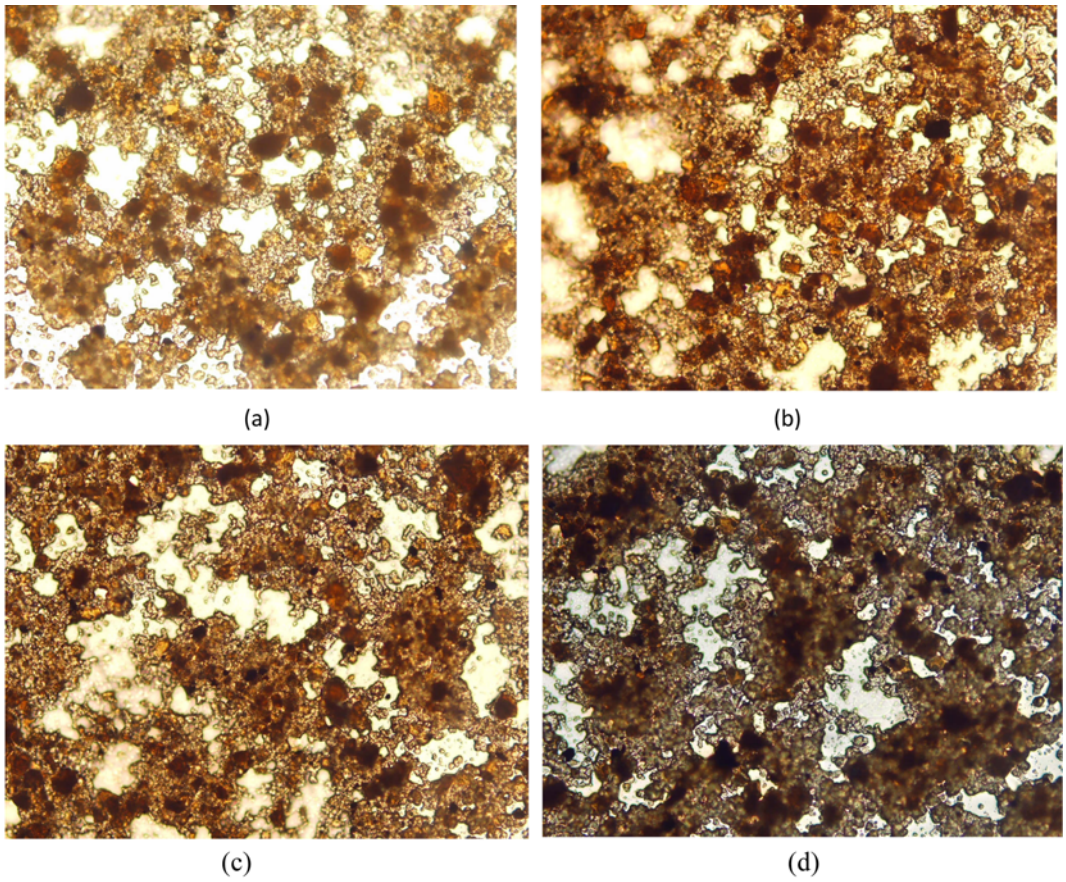

Fig. 3. The SOM images of prepared membranes containing 8%wt iron-oxide nanoparticles with various thickness of deposited Ag nanolayer thickness on membrane surface; (a) 0.0 nm, (b) 5 nm, (c) 10 nm, (d) 20 nm.

(stellar spots) is clearly seen in the SEM images. As seen in SEM images, the distribution of silver particles was improved on the membrane surface with Ag nanolayer thickness increasing. Moreover, as shown in SEM images the membrane roughness declined by the increase of nanolayer thickness coating. Deposited silver nanoparticles occupy the cracks and fissures on the membrane surface and improve the membrane selectivity. Also, membrane coating by Ag nanolayer enhances the electrical conductivity of prepared membranes (Fig. 5) sharply. The presence of more conducting region on the membrane surface can strengthen the intensity of uniform electrical field around the membrane and decrease the concentration polarization phenomenon.

2. The Effect of Ag Nanolayer Thickness on Performance of Prepared Membranes (PVC-Fe_2NiO_4 Nanoparticles Entrapped)

Obtained results (Fig. 6) revealed that membrane potential initially declined with increase of Ag nanolayer thickness up to 5 nm in prepared membranes. This may be attributed to decrease in accessibility of ion exchange functional groups in the membrane matrix because of their isolation by Ag nanoparticles which occupy the spaces around resins and so reduce the accessibility of ion exchange functional groups by their isolation. Moreover, a decrease in membrane surface charge density (Fig. 6) decreases the membrane potential. The membrane potential is increased again with more increase in nanolayer thickness from 5 to 30 nm. This is attributed to increase of density and uniform distribution of silver nanoparticles on the membrane surface (SEM images, Fig. 4), which enhances the membrane surface charge density and so provides additional conducting regions for the membrane. This causes superior interaction between ions and surface of membrane, which in turn facilitates the ion transportation between the solution and membrane phase and leads to enhanced Donnan exclusion that is responsible for the increment of membrane potential.

The permselectivity and transport number of membranes are also depicted in Fig. 7. At first, both decreased with increase of Ag nanolayer thickness to 5 nm due to lower membrane fixed ion concentration (because of ionic sites isolation by silver particles), which facilitates the co-ion percolation through the membrane and reduces the selectivity. Permselectivity and transport number were increased again with more increment of Ag nanolayer thickness from 5 to 30 nm. This happening can be explained with respect to the increase in membrane charge density with improved control of pathways for ion traffic. Moreover, with the increase of nanolayer thickness, the ionic pathways in the membrane matrix are occupied by the particles and so they are narrowed by them as space limiting factors. This causes the strengthening of the ionic sites domination on ion traffic and improves the membrane permselectivity. Furthermore, as shown in SEM images (Fig. 4), a decrease in membrane roughness at high nanolayer thickness decreases the ion interactions with membrane surface and so reduces the co-ion percolation through the membrane and increases the selectivity.

The results (Fig. 8) show that the ionic permeability and flux of ions increased initially with increase of deposited nano silver layer

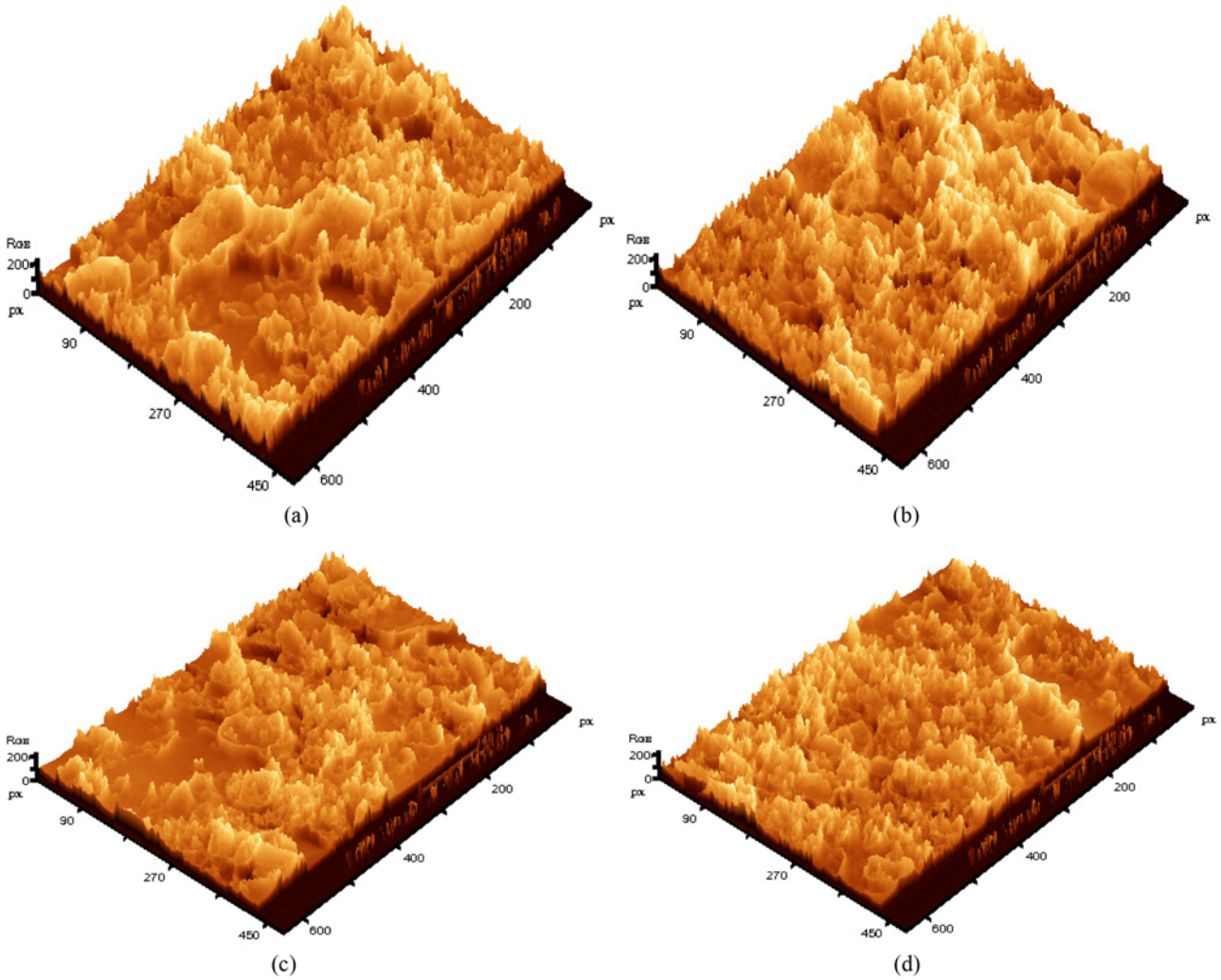

Fig. 4. 3D SEM images of prepared membranes with various deposited Ag nanolayer thickness; (a) 0.0 nm Ag-nanolayer; (b) 5 nm; (c) 10 nm; (d) 20 nm (Membrane surface coating, cracks and channels occupying by the Ag nanoparticles).

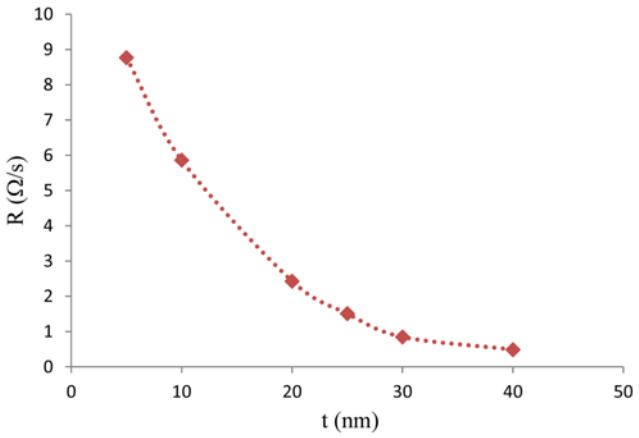

Fig. 5. The effect of Ag nanolayer coating on membrane sheet resistance at different nanolayer thickness.

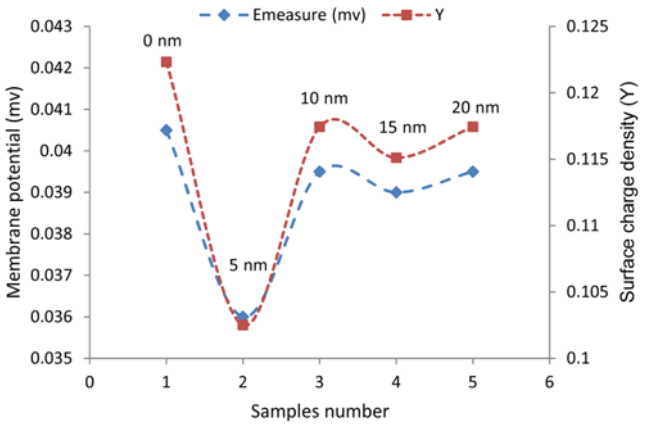

Fig. 6. Membrane potential and membrane surface charge density of prepared membranes with various thickness of deposited Ag nanolayer.

thickness up to 5 nm in prepared membranes. This is attributed to membranes' electrical property improvement (Fig. 5) by Ag nanolayer coating, which increases the intensity of the uniform electrical field around the membrane and so enhances the permeability and flux. The ionic permeability and flux decreased again with more increase in deposited nano silver layer thickness from 5 to 10 nm.

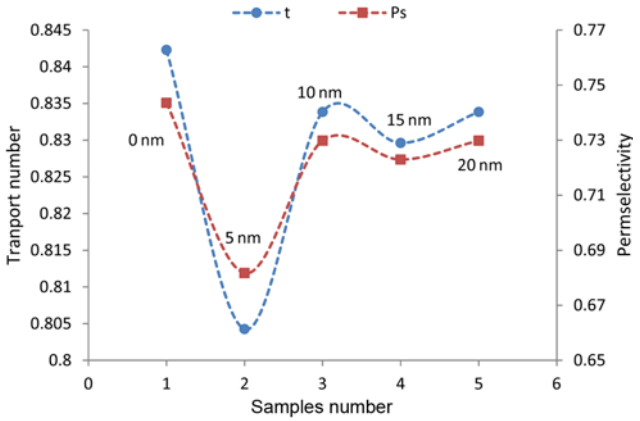

Fig. 7. Permselectivity and transport number of unmodified membrane (without Ag nanolayer coating) and modified membranes with various deposited Ag nano layer thickness (nm) on membrane surface.

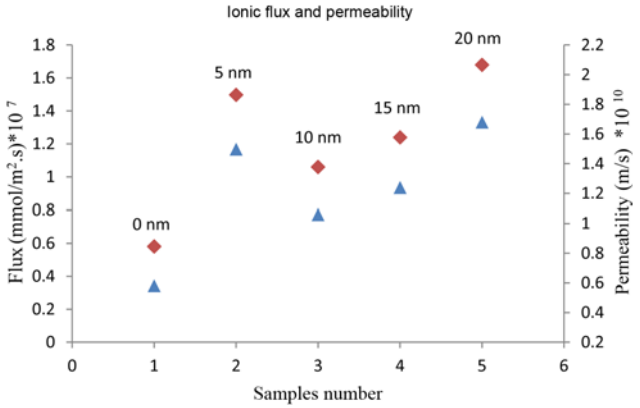

Fig. 8. Membrane permeability and flux of unmodified membrane (without Ag nanolayer coating) and modified membranes with various deposited Ag nano layer thickness (5, 10, 15, 20 nm) on membrane surface.

This decrease in permeability and flux is attributed to the formation of narrow ionic transfer channels in the membrane matrix by Ag nanoparticles occupying and filling, which reduces the ion transportation.

The permeability and flux were increased again with more increase in nanolayer thickness from 10 to 30 nm due to increase in surface charge density and also the superior electrical property of coated membranes (Fig. 5), which results in better conducting regions for the membrane and increases the intensity of uniform electrical field around the membrane, which improves the ionic permeability and flux.

3. Antibacterial Effect

The optical density (OD) was measured in three separate cells containing 1,000 CFU/m·lit (colony forming unit) of E-Coli. One of the cells was a control unit (without any membrane), which gives the growth rate of E-Coli. Fig. 9 shows the variation of optical density against time (growth rate) in the cells. Increasing the coating thickness of silver nanolayer obviously led to OD reduction. The membranes showed good ability in E-Coli removal. At higher film thickness the release of Ag particles from substrate (membrane)

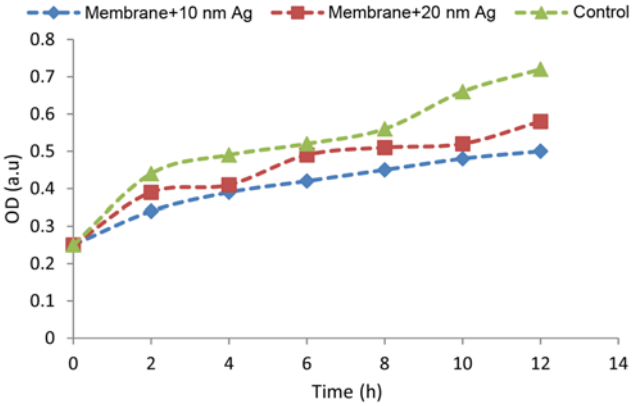

Fig. 9. The effect of deposited Ag nanolayer on growth curves of E-coli via time (investigation of membrane anti-bacterial effect).

Table 1. A typically comparison between the pristine membrane, membrane containing 8%wt Fe_2NiO_4 nanoparticles and treated membrane containing 8%wt Fe_2NiO_4 nanoparticles and 20 nm Ag nanolayer coating

Membrane	Permselectivity (%)	Flux (mmol/m^2·s)*10^8)
Pristine membrane	72	6.0
Membrane containing nanoparticles (8%wt Fe_2NiO_4)	75	5.8
Superior membrane (8%wt Fe_2NiO_4 and 20 nm Ag nanolayer)	73	16.8

may have a negative effect (toxicity to human cells). This is one of the important advantages of using magnetron sputtering for deposition of Ag nanolayer.

4. Superior Membrane

A typical comparison between the pristine membrane (without Fe_2NiO_4 nanoparticles and Ag nanolayer coating), membrane containing 8%wt Fe_2NiO_4 nanoparticles and treated membrane containing 8%wt Fe_2NiO_4 nanoparticles and 20 nm Ag nanolayer coating was carried out to investigate the ability of the treated membrane. The results in Table 1 show good electrochemical properties for the modified membrane (superior membrane) compared to others.

CONCLUSION

SEM images showed that the distribution of silver particles was improved on the membrane surface by Ag nanolayer thickness increasing. Moreover, as shown in SEM images membrane roughness declined by increase of nanolayer thickness coating. The electrical conductivity of prepared membranes was enhanced sharply by the increase in nanolayer thickness. Obtained results revealed that membrane potential, membrane surface charge density, transport number and selectivity declined initially by Ag nanolayer coating up to 5 nm in prepared membranes, and then showed increasing trend with more nanolayer thickness increasing from 5 to 30 nm. Ionic permeability and flux increased initially by silver nanolayer coat-

ing up to 5 nm in prepared membranes. The ionic permeability and flux decreased again with more increase in deposited nano layer thickness from 5 to 10 nm. Permeability and flux increased another time by more increase in nanolayer thickness from 10 to 30 nm. The membranes showed good ability in E-Coli removal. Results showed good electrochemical properties for the 20 nm Ag nanolayer coated membrane containing 8%wt iron oxide nanoparticles compared to others.

ACKNOWLEDGEMENT

The authors gratefully acknowledge ***Arak University*** and also ***Iran Nanotechnology Initiative Council*** for the financial support during this research.

REFERENCES

1. R. W. Baker, *Membrane technology and applications*, 2nd Ed. Wiley Ltd., England (2004).
2. S. M. Hosseini, S. S. Madaeni, A. R. Heidari and A. R. Moghadassi, *Desalination*, **279**, 306 (2011).
3. K. Hideo, K. Tsuzura and H. Shimizu, *Ion exchange membranes*, in: K. Dorfner (Ed.), Ion Exchangers, Walter de Gruyter, Berlin (1991).
4. H. Strathmann, *Electrodialysis and related processes*, in: R. D. Nobe, S. A. Stern (Eds.), Membrane Separation Technology-Principles and Applications, Elsevier Science, 214 (1995).
5. T. Sata and W. Yang, *J. Membr. Sci.*, **206**, 31 (2002).
6. Y. Kubuchi, H. Motomura, Y. Noma and F. Hanada, *J. Membr. Sci.*, **27**, 173 (1986).
7. T. Sata, *New application of ion-exchange membranes, in*: J. Kohovec (Ed.), Macromolecules, VSP, Utrecht, The Netherlands, 451 (1992).
8. G. S. Gohil, V. V. Binsu and V. K. Shahi, *J. Membr. Sci.*, **280**, 210 (2006).
9. P. V. Vyas, P. Ray, S. K. Adhikary, B. G. Shah and R. Rangarajan, *J. Colloid Interface Sci*., **257**, 127 (2003).
10. S. M. Hosseini, S. S. Madaeni and A. R. Khodabakhshi, *J. Appl. Polym. Sci*., **118**, 3371 (2010).
11. S. M. Hosseini, S. S. Madaeni, A. R. Heidari and A. Amirimehr, *Desalination*, **284**, 191 (2012).
12. V. K. Shahi, S. K. Thampy and R. Rangarajan, *J. Membr. Sci.*, **158**, 77 (1999).
13. J. Kerres, W. Cui, R. Disson and W. Neubrand, *J. Membr. Sci.*, **139**, 211 (1998).
14. S. Pourjafar, A. Rahimpour and M. Jahanshahi, *J. Ind. Eng. Chem.*, **18**, 1398 (2012).
15. Z. M. Liu, Z. K. Xu, L. S. Wan, J. Wu and M. Ulbricht, *J. Membr. Sci.*, **249**, 21 (2005).
16. M. G. Yan, L. Q. Liu, Z. Q. Tang, L. Huang, W. Li, J. Zhou, J. S. Gu, X. W. Wei and H. Y. Yu, *Chem. Eng. J.*, **145**, 218 (2008).
17. H. Y. Yu, Y. J. Xie, M. X. Hu, J. L. Wang, S. Y. Wang and Z. K. Xu, *J. Membr. Sci.*, **254**, 219 (2005).
18. T. Sardohan, E. Kir, A. Gulec and Y. Cengeloglu, *Sep. Purif. Technol.*, **74**, 14 (2010).
19. S. M. Hosseini, S. S. Madaeni, A. R. Khodabakhshi and A. Zendehnam, *J. Membr. Sci.*, **365**, 438 (2010).
20. E. S. Wiks, Industrial Polymers Handbook: Products, Processes, Application, Wiley-VCH Press, Germany (2001).
21. J. E. Mark, Polymer Data Handbook, Oxford University Press, New York (1999).
22. C. A. Harper, Handbook of Plastic and Elastomers, McGraw-Hill, New York (1975).
23. L. Erertovr, Physics of Thin Films, Plenum Press, 2nd Ed. (1986).
24. K. Chaloupka, Y. Malam and A. M. Seifalian, *Trends Biotechnol.*, **28**, 580 (2010).
25. I. Sondi and B. Salopek-Sondi, *J. Colloid Interface Sci*., **275**, 177 (2004).
26. D. Wei, W. Sun, W. Qian, Y. Ye and X. Ma, *Carbohyd. Res.*, **344**, 2375 (2009).
27. B. Tang, J. Wang, S. Xu, T. Afrin, W. Xu, L. Sun and X. Wang, *J. Colloid Interface Sci*., **356**, 513 (2011).
28. X. Li, Z. Wang, H. Lu, C. Zhao, H. Na and C. Zhao, *J. Membr. Sci*., **254**, 147 (2005).
29. R. K. Nagarale, V. K. Shahi, S. K. Thampy and R. Rangarajan, *React. Funct. Polym.*, **61**, 131 (2004).
30. R. K. Nagarale, G. S. Gohil, V. K. Shahi and R. Rangarajan, *Colloids Surf. A: Physicochemical and Engineering Aspects*, **251**, 133 (2004).
31. D. R. Lide, CRC Handbook of Chemistry and Physics, 87th Ed., CRC press, Boca Raton, FL (2006-2007).